Extra Linker Incorporated Zr-based MOFs for Efficient Separation of C_2 Hydrocarbons from CH_4

Chunlian Hao [a], Houyu Zhu [b], Hao Ren [c], Yuhua Chi [d], Wen Zhao [e],

Wenyue Guo [f, *]

School of Materials Science and Engineering, China University of Petroleum, Qingdao, Shandong 266580, China

[a] haocl@s.upc.edu.cn, [b] hyzhu@upc.edu.cn, [c] renh@upc.edu.cn, [d] chiyuhua@upc.edu.cn,

[e] zhaowen@upc.edu.cn, [f, *] wyguo@upc.edu.cn

* Corresponding author e-mail: wyguo@upc.edu.cn

Abstract. Exploring stable adsorbents for efficiently separating C_2 hydrocarbons from CH_4 is of importance to obtain upgraded natural gas and high-purity C_2 hydrocarbons. Here, we selected the stable Zr-based PCN-606 and the corresponding multivariate structures PCN-606-BDC, PCN-606-TPDC, and PCN-606-BDC-TPDC as the adsorbents. Their separation performances of C_2 hydrocarbons from CH_4 were investigated using GCMC simulations, revealing that the incorporation of different linkers led to a great influence on C_2/CH_4 separation. PCN-606 and PCN-606-TPDC exhibit the best C_2H_2/CH_4 separation performances with values of 46.5 and 82.5 at low pressures, and PCN-606-BDC-TPDC exhibits the largest C_2H_6/CH_4 selectivity of 30.7. The C_2H_2 adsorption relies more on Coulomb interaction between C_2H_2 and terminal -OH groups in Zr_6-clusters, whereas C_2H_4 and C_2H_6 adsorption are closely related to non-Coulomb interaction. This work highlights the potential of multivariate PCN-606 materials as excellent candidates for C_2/CH_4 separation.

Keywords: CH_4; High-purity C_2 Hydrocarbons; Multivariate PCN-606 Materials.

1. Introduction

Methane (CH_4), the major contributor of natural gas, is of abundance and environmentally friendly and has been considered a promising alternative to petroleum-based fuels [1]. The existence of impurities, such as light hydrocarbons, H_2O, CO_2, etc., could devalue CH_4. Moreover, C_2 hydrocarbons (C_2H_2, C_2H_4, and C_2H_6) are also important chemical feedstocks with high purity for manufacturing major industrial polymers. Therefore, efficient separation of C_2 hydrocarbons from CH_4 is required and is of significance for producing high-quality CH_4-based fuels and C_2 hydrocarbon gases. Compared with the traditional separation methods (such as cryogenic distillation), adsorptive separation based on porous solid adsorbents has been regarded as a potential alternative owing to the cost-saving and energy-efficiency characteristics.

MOFs have shown the possibility of adsorbate separation and purification by virtue of the high surface/pore volume and adjustable pore size/shape/surface chemistry [2]. Until now, reported MOFs with excellent separation performance are mainly attributed to the generation of strong bonding sites for one special gas, such as open metal sites (OMSs) [3]. However, although OMS-based MOFs exhibit efficient separation for light hydrocarbons, the lowered stability after activation and a strong affinity with water molecules limit their practical application [2]. Many MOFs with stable structures have been reported, but their poor adsorption and separation performances cannot satisfy the industrial requirements. This challenge has motivated researchers to develop new MOFs with stable frameworks and good separation performances.

Researchers attribute the excellent stability of Zr-MOFs to high connectivity of Zr_6-clusters and strong bond affinity between Zr^{4+} ions and COO-based ligands [4]. Most reported Zr-MOFs feature large pore sizes, which exhibit the potential of high adsorption capacities but poor separation efficiency due to the co-adsorption [5]. Therefore, simple Zr-MOFs with large pore structures cannot satisfy the requirements for efficient gas separation [6]. To obtain suitable Zr-MOF adsorbents, a

stepwise synthetic method named sequential linker installation is developed and has been successfully performed to gain various MOFs with controllable pore structures and emerging properties in gas adsorption and separation [7]. For example, Sun group obtained functionalized UPC-200(Al) with high amounts and uptake ratio (2.6) for C_2H_2/CO_2 from among 25 different multivariate UPC-200 structures with the regulation for pore size and environments, showing a benchmark fertility for C_2H_2/CO_2 [6].

Inspired by the above consideration, we chose Zr-MOFs, multivariate PCN-606 series, as the adsorbents due to excellent stability and suitable pore structure accepting different linkers [8]. The parent PCN-606 contains two pockets with different sizes, which potentially allows the installation of two lingers with the corresponding lengths, thus the incorporation of BDC and TPDC into PCN-606 leads to the formation of PCN-606-BDC, PCN-606-TPDC, and PCN-606-BDC-TPDC, respectively [8]. GCMC calculations were performed to calculate the adsorption performance of C_{1-2} hydrocarbons and separation performance of C_2/CH_4 mixtures. The results show that the incorporation of linkers into Zr-MOFs is a feasible way to construct novel adsorbents for efficient C_2/CH_4 separation.

2. Simulation Details

2.1 Models

The crystal data of the multivariate PCN-606 series were obtained from the available experimental crystallographic data [8], as shown in Fig. 1. All models were optimized by Forcite module of Material Studio with the potential parameters of universal force field (UFF) [9]. The structure properties of PCN-606 materials were calculated by Poreblzer with the helium probe molecule [10], and Table 1 gives the related parameters. Compared with PCN-606, the incorporation of BDC linker leads to a little influence on pore size but a decrease in S_A and V_P. In contrast, incorporating TPDC linker into PCN-606 significantly decreases the pore sizes and increases the surface areas and pore volumes, which could provide more interaction surfaces for adsorbing more gas molecules.

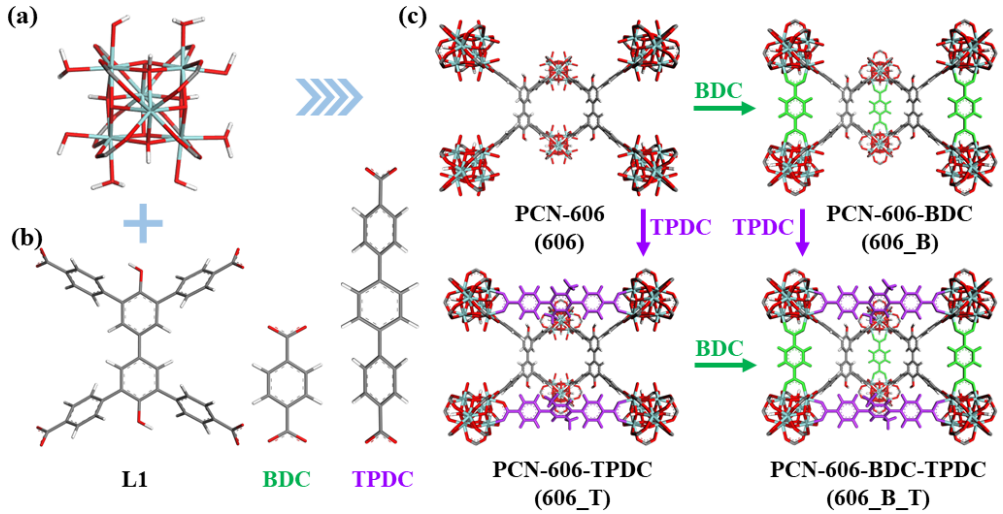


Fig 1. The structures of Zr_6 cluster, organic ligands, and multivariate PCN-606 materials in this work.

Table 1. Structure properties of PCN-606 materials in this work.

	ρ [a]	D_L [b]	D_M [b]	S_A [c]	V_P [d]
PCN-606	0.6	12.1	13.5	1944.3	0.7
PCN-606-BDC	0.7	11.4	13.5	1796.5	0.6
PCN-606-TPDC	0.7	7.4	11.2	2317.5	0.9
PCN-606-BDC-TPDC	0.7	7.5	11.0	2087.7	0.9

Unit: [a] g cm^{-3}; [b] Å; [c] m^2 g^{-1}; [d] cm^3 g^{-1}

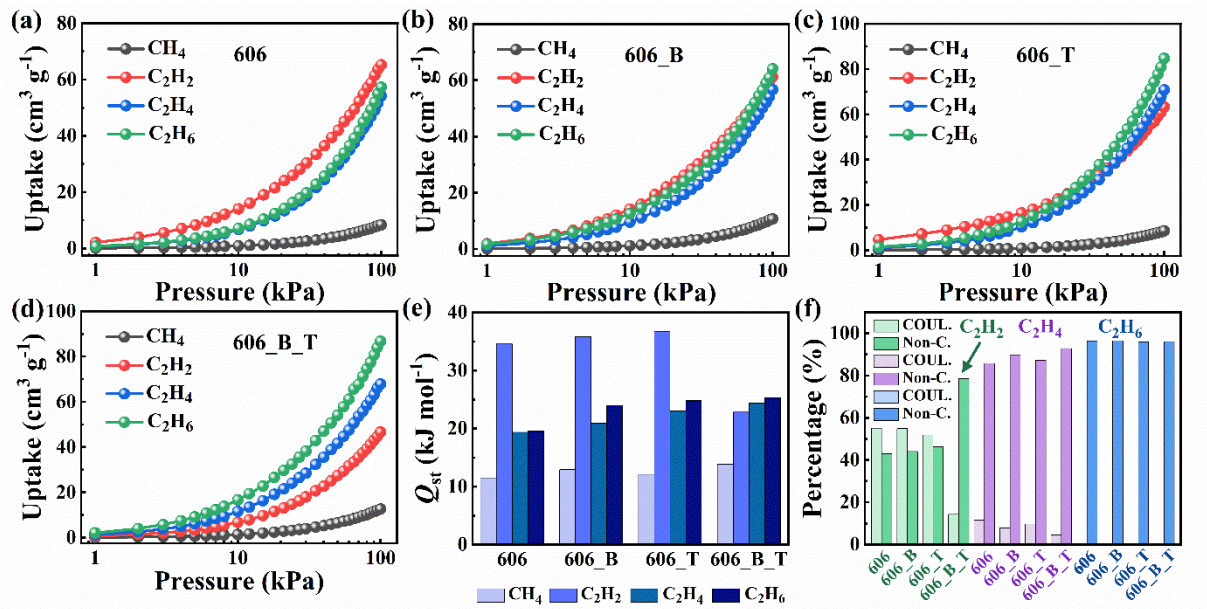
2.2 Simulation Details

GCMC simulations were performed to calculate the adsorption of pure gases and the selectivity of binary mixtures in PCN-606 materials. All MOFs and adsorbates (including C_2H_2, C_2H_4, C_2H_6, and CH_4) were kept rigid during GCMC simulations [11], and periodic boundary conditions were applied in all three dimensions. The L-J and electrostatic interactions were combined to describe the interactions of gas-gas and gas-framework. UFF and Dreiding [12] force fields were used to describe the MOF structures. L-B mixing rules were applied to describe the L-J parameters between two diverse interacting sites. All GCMC calculations were obtained by the music code [13]. DFT calculations were applied to calculate the atomic partial charges as the important input parameters using Dmol^3 module. Generalized gradient approximation (GGA) with the Perdew-Burke-Ernzerhof (PBE) functional was used to do all-electron spin-unrestricted DFT calculations.

3. Results and Discussions

3.1 Single-component Gas Adsorption

Fig. 2a-d presents the absolute adsorption isotherms of various adsorbates in PCN-606 materials at 298 K and up to 100 kPa. The C_2 uptakes are obviously larger than those of CH_4 among all PCN-606 materials over the whole pressure range considered, which is attributed to the lower polarizability of CH_4. As shown in Fig. 2a, the uptakes of C_2 hydrocarbons in parent PCN-606 follow the order of C_2H_2 (65.3) > C_2H_4 (57.3) > C_2H_6 (54.2) with the uptakes in cm^3 g^{-1} at 100 kPa in the parentheses.



(a-d) Adsorption isotherms (e) Adsorption heats (f) Average percentages of non- and Coulomb interactions

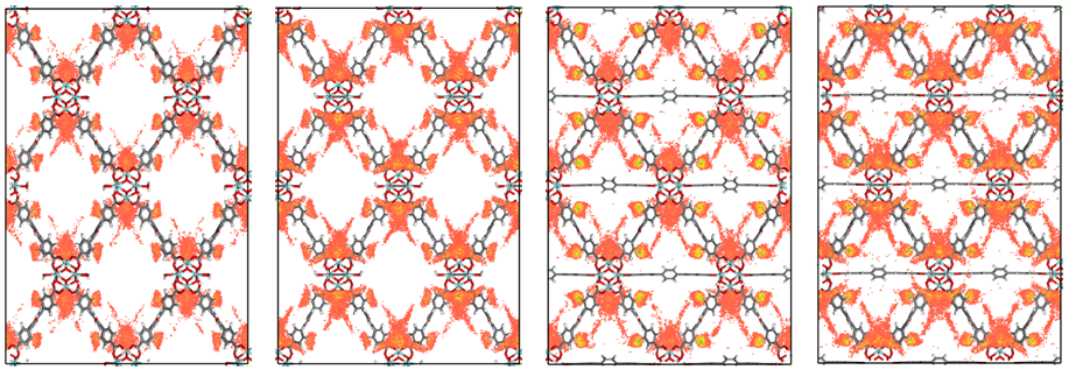
Fig 2. The adsorption isotherms, adsorption heats, and the average percentages of non- and Coulomb interactions for gas adsorption in PCN-606 materials at 298 K

After introducing the BDC linker, the uptakes of C_2H_4 and C_2H_6 increase and are comparable with that of C_2H_2. After the incorporation of the TPDC linker, the uptakes of C_2H_4 and C_2H_6 increase further, but the C_2H_2 uptakes decrease obviously, especially in PCN-606-BDC-TPDC. The corresponding uptakes of C_2H_2, C_2H_4, and C_2H_6 at 100 kPa are 64.0, 61.2, and 56.6 cm^3 g^{-1} in PCN-606-BDC, 63.2, 70.8, and 87.4 cm^3 g^{-1} in PCN-606-TPDC, and 46.6, 67.8, and 86.7 cm^3 g^{-1} in PCN-606-BDC-TPDC.

Fig. 2e presents the adsorption heats of CH_4 and C_2 hydrocarbons in PCN-606 materials at 298 K. The Q_{st} of CH_4 is smaller than those of C_2 hydrocarbons, with the same order of their adsorption

uptakes in PCN-606 materials. The Q_{st} of C_2H_2 is obviously larger than those of C_2H_4 and C_2H_6 in PCN-606, PCN-606-BDC, and PCN-606-TPDC, and the incorporation of BDC and TPDC makes the adsorption heats of C_2H_6 obviously larger than $Q_{st}(C_2H_4)$. Whereas in PCN-606-BDC-TPDC, the Q_{st} of C_2 hydrocarbons follows the order of $Q_{st}(C_2H_6) > Q_{st}(C_2H_4) > Q_{st}(C_2H_2)$, consistent with the trend of C_2 hydrocarbon uptakes. To deeply understand the gas-framework interactions during the adsorption of gases, the average percentages of Coulomb and non-Coulomb interactions between gases and frameworks are provided in Fig. 2f. For C_2H_2 adsorption, the average percentage of Coulomb interaction is larger than that of non-Coulomb interaction in the parent, BDC, and TPDC incorporated PCN-606 materials, whereas shows the reverse order in PCN-606-BDC-TPDC. It is attributed to that the incorporation of both BDC and TPDC into PCN-606 entirely replaces the terminal -OH groups in Zr_6 clusters, which serve as the important adsorption sites for C_2H_2 through C-H···O hydrogen bindings and have been verified by our previous work. For C_2H_4 adsorption, the percentages of Coulomb interaction are significantly smaller than those of non-Coulomb interaction in PCN-606 materials. Unlike the above situations, C_2H_6 adsorption only depends on non-Coulomb interaction in all PCN-606 materials.

The density distributions are investigated to further understand the adsorption progresses of CH_4 and C_2 hydrocarbons in PCN-606 materials, and Fig. 3 provides the density distributions of C_2H_2 adsorption, which is shown as the representative for other gases due to the similar adsorption situations in PCN-606 materials. As shown in Fig. 3a, C_2H_2 molecules mainly accumulate in framework surfaces in PCN-606, especially around the Zr_6 clusters, which is similar to C_2H_2 adsorption in PCN-606-BDC. However, owing to the great influence of TPDC on PCN-606 structure, the incorporation of TPDC leads to a great influence on C_2H_2 adsorption, showing that C_2H_2 molecules tend to accumulate in the regions surrounded by Zr_6 cluster and three different linkers (Fig. 3c, d).



(a) 606−C_2H_2 **(b) 606_B−C_2H_2** **(c) 606_T−C_2H_2** **(d) 606_B_T−C_2H_2**

Fig 3. Density distributions of C_2H_2 on PCN-606 materials at 298 K and 100 kPa.

3.2 Separation of Gas Mixtures

The visible differences in adsorption heats and amounts between C_2 hydrocarbons and CH_4 demonstrate the potential of selectively separating C_2/CH_4 mixtures. Fig. 4 provides the adsorption selectivities of equimolar C_2/CH_4 mixtures in PCN-606 materials at 298 K, showing the significant effects of introducing different linkers on C_2/CH_4 separation. The C_2H_2/CH_4 separation is more related to the incorporation of various linkers: the C_2H_2/CH_4 selectivity (46.5) in PCN-606 increases to 82.5 in PCN-606-TPDC at low pressures, but decreases to 26.1 and 9.5 in PCN-606-BDC and PCN-606-BDC-TPDC at same conditions. Thereinto, the C_2H_2/CH_4 selectivities in PCN-606 and PCN-606-TPDC decrease exponentially due to the quick decline of C_2H_2-framework interactions, and the analogous phenomenon has been seen in many reported MOFs [14]. After the incorporation of BDC and TPDC linkers, the selectivities of C_2H_4/CH_4 and C_2H_6/CH_4 increase to 13.8-15.4 for C_2H_4/CH_4 and 25.0-30.7 for C_2H_6/CH_4 at 100 kPa, compared with those in parent PCN-606 (13.1 and 15.0 for C_2H_4/CH_4 and C_2H_6/CH_4). Therefore, PCN-606 and PCN-606-TPDC reveal the potential of

C_2H_2/CH_4 separation with low C_2H_2 concentrations, and PCN-606-BDC-TPDC shows the potential for C_2H_6/CH_4 separation.

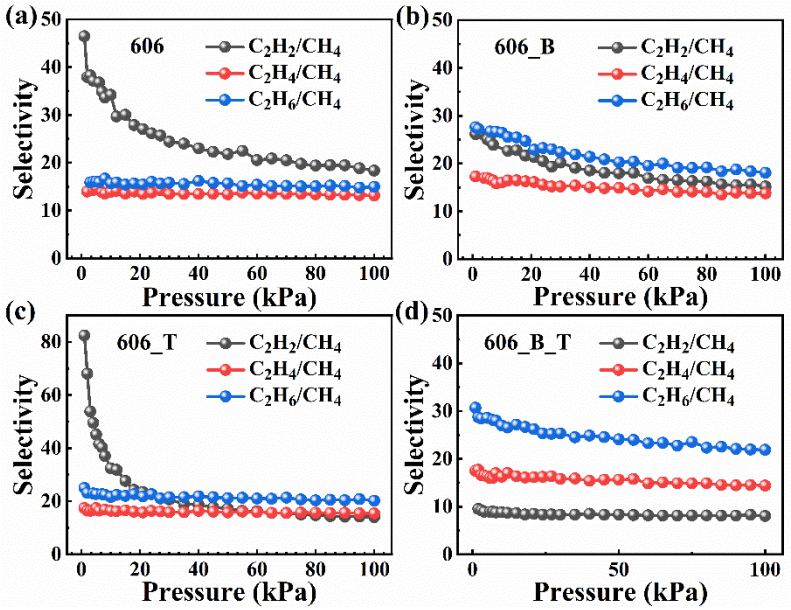


Fig 4. The C_2/CH_4 selectivities of PCN-606 materials at 298 K

4. Conclusion

In summary, effects of the incorporation of BDC and TPDC linkers in stable Zr-based PCN-606 on selectively separating C_2 hydrocarbons over CH_4 have been systematically investigated by GCMC simulations, showing that the incorporation of different linkers leads to a great change in framework structures. Thereinto, PCN-606 and PCN-606-TPDC exhibit the best C_2H_2/CH_4 separation performances with values of 46.5 and 82.5 at low pressures, and the simultaneous incorporation of BDC and TPDC in PCN-606 makes the differences between C_2/CH_4 selectivity clearly differentiated, accompanied by the largest C_2H_6/CH_4 selectivity of 30.7. The C_2H_2 adsorption relies more on Coulomb interaction through interacting with terminal -OH groups in Zr_6 clusters, whereas non-Coulomb interaction plays a crucial effect on C_2H_4 and C_2H_6 adsorption. This work highlights the potential of multivariate PCN-606 materials as excellent candidates for C_2/CH_4 separation. Based on the above results, we would further investigate C_2/CH_4 separation performances in multivariate MOFs through exquisite control over pore size and pore chemistry.

Acknowledgments

Our work was supported in financial terms by Taishan Scholars Program of Shandong Province (tsqn201909071) and the Fundamental Research Funds for the Central Universities (19CX05001A, 20CX05010A, and 05Y19080021).

References

[1] Ma, X., Liu, B., Wu, Q., Li, D., Chen, R., Zeng, Z., Li, L. (2021) Specific Li^+ sites in a nanoporous carbon for enhanced light hydrocarbons storage and separation: GCMC and DFT simulations. Fuel, 288: 119647.

[2] Hao, C., Ren, H., Zhu, H., Chi, Y., Zhao, W., Liu, X., Guo, W. (2022) CO_2-favored metal–organic frameworks SU-101(M) (M = Bi, In, Ga, and Al) with inverse and high selectivity of CO_2 from C_2H_2 and C_2H_4. Sep. Purif. Technol., 290: 120804.

[3] Geng, S., Lin, E., Li, X., Liu, W., Wang, T., Wang, Z., Sensharma, D., Darwish, S., Andaloussi, Y., Pham, T., Cheng, P., Zaworotko, M., Chen, Y., Zhang, Z. (2021) Scalable room-temperature synthesis of highly

robust ethane-selective metal–organic frameworks for efficient ethylene purification. J. Am. Chem. Soc., 143: 8654-8660.

[4] Yuan, S., Feng, L., Wang, K., Pang, J., Bosch, M., Lollar, C., Sun, Y., Qin, J., Yang, X., Zhang, P., Wang, Q., Zou, L., Zhang, Y., Zhang, L., Fang, Y., Li, J., Zhou, H.C. (2018) Stable metal-organic frameworks: Design, synthesis, and applications. Adv. Mater., 30: 1704303.

[5] Chen, B., Pei, J., Wen, H.M., Gu, X.W., Qian, Q.L., Yang, Y., Cui, Y., Li, B., Qian, G. (2021) Dense packing of acetylene in a stable and low-cost metal–organic framework for efficient C_2H_2/CO_2 separation. Angew. Chem. Int. Ed., 60: 25068-25074.

[6] Fan, W., Yuan, S., Wang, W., Feng, L., Liu, X., Zhang, X., Wang, X., Kang, Z., Dai, F., Yuan, D., Sun, D., Zhou, H.C. (2020) Optimizing multivariate metal-organic frameworks for efficient C_2H_2/CO_2 separation. J. Am. Chem. Soc., 142: 8728-8737.

[7] Chen, C., Wei, Z., Jiang, J., Zheng, S., Wang, H., Qiu, Q., Cao, C., Fenske, D., Su, C. (2017) Dynamic spacer installation for multirole metal-organic frameworks: A new direction toward multifunctional MOFs achieving ultrahigh methane storage working capacity. J. Am. Chem. Soc., 139: 6034-6037.

[8] Pang, J., Yuan, S., Qin, J., Wu, M., Lollar, C., Li, J., Huang, N., Li, B., Zhang, P., Zhou, H. (2018) Enhancing pore-environment complexity using a trapezoidal linker: Toward stepwise assembly of multivariate quinary metal-organic frameworks. J. Am. Chem. Soc., 140: 12328-12332.

[9] Rappe, A.K., Casewit, C.J., Colwell, K.S., Goddard, W., Skiff, W. (1992) UFF, A full periodic table force field for molecular mechanics and molecular dynamics simulations. J. Am. Chem. Soc., 114: 10024-10035.

[10] Amp, L.S., Harrison, A. (2011) Computational structure characterisation tools in application to ordered and disordered porous materials. Mol. Simulat., 37: 1248-1257.

[11] Gu, C., Liu, J., Hu, J., Wu, D. (2020) Metal-organic frameworks chelated by zinc fluorides for ultra-high affinity to acetylene during C_2/C_1 separations. Fuel, 266: 117037.

[12] Mayo, S.L., Olafson, B.D., Goddard, W.A. (1990) DREIDING: A generic force field for molecular simulations. J. Phys. Chem., 94: 8897-8909.

[13] Gupta, A., Chempath, S., Sanborn, M.J., Clark, L.A., Snurr, R.Q. (2003) Object-oriented programming paradigms for molecular modeling. Mol. Simulat., 29: 29-46.

[14] Zhang, F., Li, K., Chen J., Zhang, X., Li, K., Shang, H., Ma, L., Guo, W., Wu, X., Yang, J., Li, J. (2022) Efficient N_2/CH_4 separation in a stable metal–organic framework with high density of open Cr sites. Sep. Purif. Technol., 281: 119951.